

## Structural redesign and stabilization of the overlapping tandem $\beta$ -turns of RNA polymerase II

JOHN R. DOBBINS<sup>1</sup>, NAGARAJAN MURALI<sup>2</sup> and ERIC C. LONG<sup>1</sup>

Departments of <sup>1</sup>Chemistry and <sup>2</sup>Physics, Indiana University Purdue University-Indianapolis, Indianapolis, Indiana, USA

Received 9 August, revised 18 September, accepted for publication 30 October 1995

Peptides representing single repeat units of the carboxy-terminal domain (CTD) of RNA polymerase II (Tyr-Ser-Pro-Thr-Ser-Pro-Ser-Tyr-NH<sub>2</sub>, **1**) contain overlapping Ser-Pro-Xaa-Xaa  $\beta$ -turn forming sites which permit their overall structure to closely resemble members of the quinoxaline class of antitumor DNA bisintercalators. We have modified this native sequence at the  $i+2$  positions of each  $\beta$ -turn unit by substituting Gly or D-Ala in an attempt to preorganize this structure in aqueous solution. CD and NMR spectroscopic investigations confirmed the presence of type II  $\beta$ -turns within each of the substituted peptides in contrast to the native sequence which contains a relatively low population of turn structure. In addition, an examination of singly substituted peptides suggests that an increase in the population of  $\beta$ -turn structure within the amino-terminal Ser-Pro-Xaa-Xaa site also increased the formation of  $\beta$ -turn structure in the carboxy-terminal (unmodified) Ser-Pro-Xaa-Xaa site; in comparison, substitution in the carboxy-terminal site did not influence structure in the remaining portion of the peptide. Overall, these results suggest that the structures formed could provide unique, preorganized linkers for the construction of novel DNA-interactive bisintercalators. © Munksgaard 1996.

**Key words:**  $\beta$ -turns; circular dichroism; DNA intercalation; RNA polymerase II; nuclear magnetic resonance

Recent investigations have uncovered several classes of DNA binding proteins that employ structural motifs (1) closely resembling antitumor natural products to assist in their association with nucleic acids [e.g. histones H1 and H2B from sea urchin sperm (2) and HMG-I/Y (3) which use peptide moieties to recognize the DNA minor groove of A/T-rich regions in a fashion similar to distamycin and netropsin (4)]. Among these examples, the individual repeat units of the carboxy-terminal domain (CTD) of RNA polymerase II (5), -(Ser-Pro-Thr-Ser-Pro-Ser-Tyr)<sub>n</sub>-, adopt an overall structure that corresponds quite closely (6) to members of the quinoxaline family (7) of antitumor *bis-intercalators* of DNA (i.e. echinomycins and triostins).

Previously, NMR studies (8) of a model peptide synthesized to mimic the environment of one repeat of the CTD (Tyr-Ser-Pro-Thr-Ser-Pro-Ser-Tyr) revealed that each Ser-Pro-Xaa-Xaa unit within this sequence adopts a low population of  $\beta$ -turn structure that permits a parallel alignment of the flanking tyrosine residues with a gap distance of ca. 10.2 Å (Fig. 1); this structure is seemingly poised for the simultaneous insertion of each aromatic side chain

between the stacked Watson-Crick base pairs of the DNA helix in a bis-intercalative fashion. Indeed, biophysical and hydrodynamic investigations of DNA binding by these individual motifs support the notion that both aromatic residues partially stack with the base pairs of the DNA helix (6, 9), an interaction of biological significance that not only alters the DNA structure (9), but may also increase

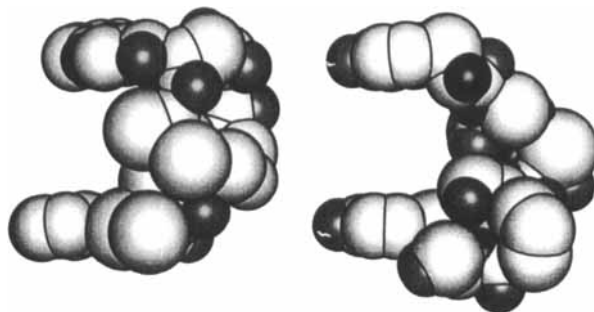


FIGURE 1  
A comparison of the structures of triostin A (left) and peptide 1 (right).

the population of  $\beta$ -turns within the CTD by utilizing the DNA as a 'scaffolding', thereby increasing the likelihood of enzymatic phosphorylation of this domain (10).

Given the uncanny structural similarities that exist between the individual repeat units of the CTD and members of the quinoxaline group of antitumor agents, our laboratories have sought to determine if a redesigned peptide motif can yield novel DNA interactive agents with a spectrum of activities and sequence selectivities different from established bis-intercalators. In addition, detailed investigations of derivatives of the repeat units of the CTD may also yield: (i) structure–function information regarding their DNA binding and recognition mechanism; (ii) structural insight pertaining to overlapping  $\beta$ -turns that could find applications in the *de novo* design of proteins and peptides; and (iii) substrate analogues as probes for the enzymes involved in the phosphorylation (11) and glycosylation (12) of the CTD.

With knowledge of the conformational flexibility of peptides representing the heptad units of the CTD in aqueous solution (8), the goal of the work presented herein was to investigate strategies leading to the structural preorganization of this motif with a *minimal* change in its peptide character. Thus, the experimentation presented has focused on the redesign of the overlapping  $\beta$ -turns that connect each aromatic amino acid along with an examination of this preorganization by both circular dichroism (CD) and two-dimensional proton nuclear magnetic resonance spectroscopy (2DNMR). Our findings indicate that conformational stability can be achieved through substitutions of key amino acids leading to unique, folded peptides and insight into the properties of tandem  $\beta$ -turn structures.

## EXPERIMENTAL PROCEDURES

*Peptide synthesis and characterization.* All peptides examined in this study were synthesized as carboxy-terminal amides through manual, solid phase protocols using commercially available starting materials and reagents (13–15). Following their synthesis, each peptide was purified by reversed-phase high-performance liquid chromatography and characterized by fast atom bombardment mass spectroscopy (FAB-MS).

*CD spectroscopy.* CD spectra were recorded at room temperature on a Jasco J720 spectropolarimeter. Peptide solutions (50  $\mu$ M) were prepared in deionized water (pH 4.2) from stocks quantitated by UV–vis spectroscopy based on tyrosine absorbance ( $\lambda_{\text{max}} = 275$  nm, pH 7.5,  $\epsilon = 1500$ ). All samples were analyzed in 0.5 cm cylindrical quartz cells, and a solvent blank was subtracted from each peptide spectrum to eliminate background interference. Each spectrum was

obtained by averaging three scans in the 250–190 nm wavelength range at a scan speed of 50 nm/min (response of 8 s/nm bandwidth of 1.0 nm and resolution of 8 s). All CD spectra are reported in mean residue ellipticity (MRE).

*NMR spectroscopy.* Samples for NMR analyses were prepared by dissolving 5 mg of solid, lyophilized peptide in 600  $\mu$ L of a 90% H<sub>2</sub>O/10% D<sub>2</sub>O solution adjusted to pH 4.2 containing ca. 0.3 mM trimethylsilylpropionic acid (TSP) solution as a standard. All NMR spectra were acquired on a Varian Unity 500 spectrometer with the sample temperature maintained at 10 °C. Phase-sensitive two-dimensional NMR experiments were employed for assignment of the peptide spectra and for detection of secondary structure in aqueous solution. All spectra were referenced with respect to TSP at 0 parts per million (ppm). Solvent signal was suppressed by applying an appropriate presaturating radiofrequency field. Quadrature detection in F<sub>1</sub> was achieved using the States hypercomplex method (16). Sequence specific assignment of each peptide was achieved using two-dimensional double quantum filtered correlated spectroscopy (DQF-COSY) (17) and two-dimensional rotating frame Overhauser spectroscopy (ROESY) (18, 19). The mixing time employed in all ROESY experiments was 250 ms, and the radiofrequency field strength used for spin locking was 4.5 kHz. In all DQF-COSY and ROESY experiments, the spectral width was 5999.7 Hz in both dimensions, and 256  $t_1$  experiments were recorded, with 2048 complex points for each free induction decay. The number of scans per  $t_1$  point was 64. Two-dimensional Fourier transformations were performed on a SUN Sparc 5 work station using shifted (90°) sine-squared weighting in both dimensions and zero-filling to 2k in F<sub>2</sub> and 2k in F<sub>1</sub>.

Temperature coefficients for the backbone amide proton chemical shifts were determined by performing several one-dimensional NMR experiments in which the sample temperature was varied between 5 and 30 °C. The chemical shift of each amide proton was plotted against temperature and in all cases the chemical shift varied linearly; the slope computed from these graphs yielded the temperature coefficients in units of parts per billion/K. (ppb/K).

*Molecular modeling.* Molecular modeling was performed on a Silicon Graphics workstation using Quanta Charrmm software. Models of **2** and **3** were constructed to include the typical backbone torsion angles of the  $i+1$  and  $i+2$  residues of type II  $\beta$ -turn structures (20) within each Ser-Pro-Xaa-Xaa site; orientation of each Ser-Pro-Xaa-Xaa relative to one another in an individual peptide was based on previous models of the native sequence found in **1** (6).

## RESULTS AND DISCUSSION

*Peptide design and synthesis*

Given the low population of  $\beta$ -turns present in a single repeat unit of the native sequence found in the CTD, our goal was to impart structural preorganization to the peptide in a fashion that *maintains* the overall steric and chemical features of this sequence. To accomplish this, two peptides were synthesized in which the  $i+2$  positions of each of the overlapping Ser-Pro-Xaa-Xaa  $\beta$ -turns were substituted with either glycine or D-alanine (Fig. 2). These substitutions are known to facilitate the formation of type II  $\beta$ -turns within model oligopeptides by removing the steric hindrance to turn formation at the  $i+2$  position (21). Synthesis of disubstituted analogues of our model of the native sequence (Tyr-Ser-Pro-Thr-Ser-Pro-Ser-Tyr-NH<sub>2</sub>, **1**) resulted in two carboxamide oligopeptides: Tyr-Ser-Pro-Gly-Ser-Pro-Gly-Tyr-NH<sub>2</sub>, **2**, and Tyr-Ser-Pro-D-Ala-Ser-Pro-D-Ala-Tyr-NH<sub>2</sub>, **3**. In addition, upon structural analyses of these analogues, two additional oligopeptides were synthesized to explore further details of the factors involved in the preorganization of these unique, overlapping  $\beta$ -turn systems. These peptides included Tyr-Ser-Pro-Gly-Ser-Pro-Ser-Tyr-NH<sub>2</sub>, **4**, and Tyr-Ser-Pro-Thr-Ser-Pro-Gly-Tyr-NH<sub>2</sub>, **5**.

*CD analysis of the disubstituted peptides.* The structures of **1–3** were evaluated using CD spectroscopy. While the exact quantitation of turn structure by CD is difficult to achieve (22), the general spectral features allow a qualitative assessment of  $\beta$ -turn formation within a family of structurally related peptides. Specifically, spectra of all peptides under the same conditions were compared as shown in Fig. 3. The spectra of **2** and **3** were found to have distinct negative ellipticities in the wavelength range  $<190$  nm and  $>220$  nm and a positive ellipticity in the 200–210 nm

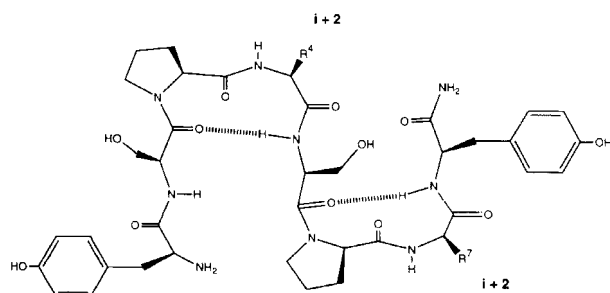
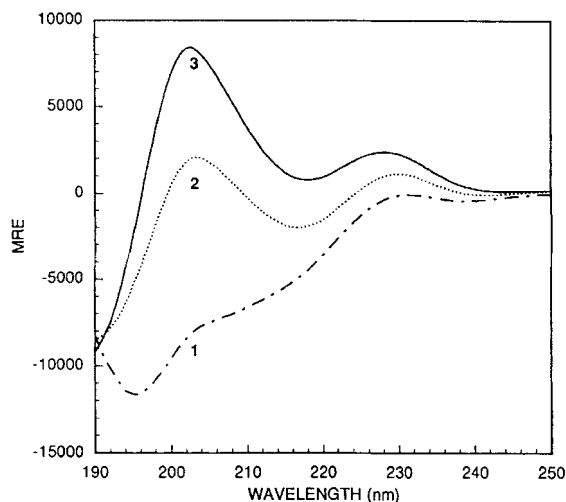


FIGURE 2

Schematic diagram of the overlapping  $\beta$ -turn system. The  $i+2$  positions of the amino-terminal Ser-Pro-Xaa-Xaa  $\beta$ -turn ( $R^4$ , left) and carboxy-terminal Ser-Pro-Xaa-Xaa  $\beta$ -turn ( $R^7$ , right) are, respectively, Thr and Ser for peptide **1**, Gly and Gly for peptide **2**, D-Ala and D-Ala for peptide **3**, Gly and Ser for peptide **4**, and Thr and Gly for peptide **5**.

FIGURE 3  
CD spectra of peptides **1**, **2**, and **3**.

range (MRE ca. 2000 and ca. 8000 deg cm<sup>2</sup> dmol<sup>-1</sup>, respectively), all of which are characteristic of type II  $\beta$ -turns (21–23). In contrast, the CD spectrum of **1**, which contains a significant negative ellipticity in the 200 nm region, suggests a secondary structure not containing type II  $\beta$ -turns; a comparison with published spectra suggests that **1** is predominately a combination of types I and II  $\beta$ -turn and random coil structure (24). These results, in agreement with previous studies (8), suggest that the amino acid substitutions selected to enforce preorganization have been successful in imparting a significant population of well defined structure to the peptide sequence.

*CD analysis of the monosubstituted peptides*

As demonstrated above, substitution of glycine or D-alanine into the native repeat sequence resulted in the formation of increasingly structured peptides most likely containing type II  $\beta$ -turns. Following this observation, the effect(s) of a single substitution within the peptide was determined to evaluate whether the formation of one  $\beta$ -turn in the tandem array influenced the conformational stability of the adjacent (unsubstituted) Ser-Pro-Xaa-Xaa site. As shown in Fig. 4, the CD spectra of **4** and **5**, which contain a *single* glycine substitution in either the amino-terminal or carboxy-terminal  $\beta$ -turn forming sites of the peptide, respectively, suggests a combination of structured and unstructured elements in solution. Specifically, in the region 200–210 nm, the ellipticity of **4** and **5** is no longer as negative as **1**, but is still somewhat reminiscent of the positive ellipticity found in **2**. These observations, in light of previously analyzed peptides (21–25), indicate that the structures of peptides **4** and **5** most likely consist of a combination of either type I  $\beta$ -turn or random coil *with* type II  $\beta$ -turns (24). This is understandable given the fact

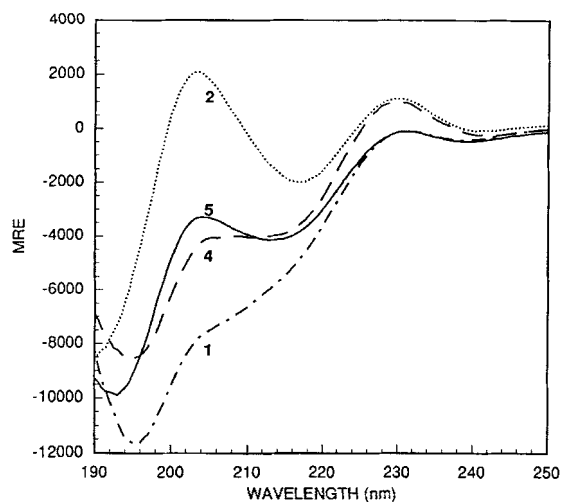


FIGURE 4  
CD spectra of peptides 4 and 5.

that glycine at the  $i+2$  position favors type II  $\beta$ -turns, while a serine or threonine at the  $i+2$  position would favor type I  $\beta$ -turns, as observed previously in the analysis of the native sequence (8). It must be noted, however, that CD analyses alone cannot determine whether the two halves of one peptide are structured uniquely vs. a population of differently folded peptides in solution. Therefore, NMR analyses were essential to further evaluate the structure of these peptides.

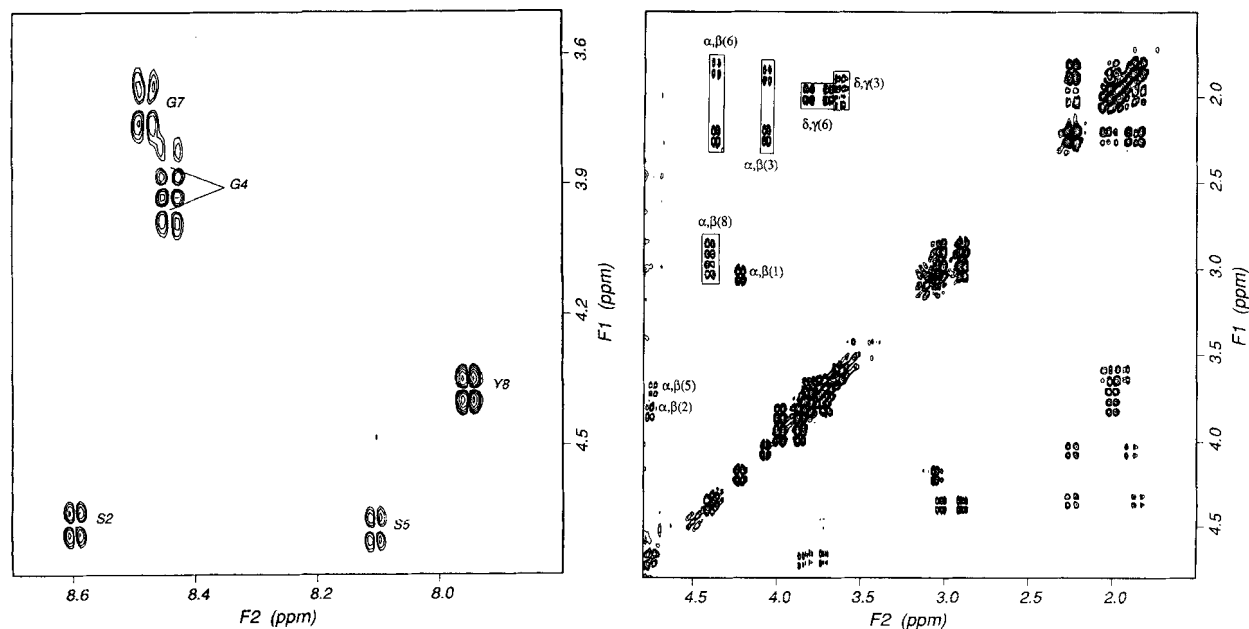


FIGURE 5  
Portions of the 500 MHz proton DQF-COSY spectrum of peptide 2 showing assignments in the NH-C $\alpha$ H region (left panel) and in the upfield region (right panel) of the spectrum.

### NMR resonance assignments

Resonance assignment of the proton spin systems of each peptide was a relatively easy task even though several residues occur repeatedly in an individual sequence. Of the six possible amide resonances within each peptide, five were observed with the missing amide resonance assigned to the amino-terminal tyrosine. Ultimately, the individual amino acid residues of each peptide were identified unambiguously from their DQF-COSY spectrum spin-pattern connectivities (e.g. peptide 2, Fig. 5). The molecular weights of all peptides examined in this study were ca. 0.8 kDa thus ROESY (18, 19) experiments were employed instead of two-dimensional nuclear Overhauser experiments (NOESY) (26). The  $d_{\alpha N}$  and  $d_{\beta N}$  connectivities observed in each ROESY spectrum were used to identify the specific position of each amino acid residue in the primary sequence. The resonance assignments for the various protons in all the peptides studied are summarized in Table 1 along with the backbone amide proton temperature coefficients and the  $^3J_{HN\alpha}$  coupling constants.

### NMR analysis of $\beta$ -turn structure

The identification of  $\beta$ -turn structures from NMR data relies on several parameters (27, 28), including: (i) specific NOE connectivities that are not usually observed in unfolded peptide structures, (ii) inter-residue hydrogen bonding of backbone amide protons as evaluated by temperature coefficient measurements, and (iii) reduced  $^3J_{HN\alpha}$  coupling constants for

TABLE I  
*Peptide resonance assignments, temperature coefficients and coupling constants<sup>a</sup>*

| Residue   | Chemical shift (ppm) |              |             |              |              |        | $\frac{\Delta\delta_{\text{NH}}}{\Delta T} \times 10^3$ | $^3J_{\text{HN}\alpha}$ |
|---|----------------------|--------------|-------------|--------------|--------------|--------|---|-------------------------|
|   | NH                   | C $\alpha$ H | C $\beta$ H | C $\gamma$ H | C $\delta$ H | Others |   |                         |
| Tyr-Ser-Pro-Thr-Ser-Pro-Ser-Tyr-NH <sub>2</sub> (1)     |                      |              |             |              |              |        |   |                         |
| Tyr <sup>1</sup>  | –                    | 4.25         | 3.13, 3.07  | –            | –            | –      | –   | –                       |
| Ser <sup>2</sup>  | 8.54                 | 4.74         | 3.86, 3.75  | –            | –            | –      | (–)7.53   | 8.0                     |
| Pro <sup>3</sup>  | –                    | 4.40         | 2.34, 2.02  | 2.02, 2.02   | 3.82, 3.82   | –      | –   | –                       |
| Thr <sup>4</sup>  | 8.23                 | 4.30         | 4.22        | –            | –            | 1.20   | (–)7.48   | 8.0                     |
| Ser <sup>5</sup>  | 8.31                 | 4.74         | 3.86, 3.78  | –            | –            | –      | (–)7.76   | 7.5                     |
| Pro <sup>6</sup>  | –                    | 4.40         | 2.22, 1.74  | 2.00, 2.00   | 3.63, 3.63   | –      | –   | –                       |
| Ser <sup>7</sup>  | 8.39                 | 4.33         | 3.74, 3.74  | –            | –            | –      | (–)7.59   | 7.0                     |
| Tyr <sup>8</sup>  | 8.16                 | 4.54         | 3.08, 2.95  | –            | –            | –      | (–)7.65   | 7.5                     |
| Tyr-Ser-Pro-Gly-Ser-Pro-Gly-Tyr-NH <sub>2</sub> (2)     |                      |              |             |              |              |        |   |                         |
| Tyr <sup>1</sup>  | –                    | 4.22         | 3.06, 3.06  | –            | –            | –      | –   | –                       |
| Ser <sup>2</sup>  | 8.60                 | 4.70         | 3.83, 3.74  | –            | –            | –      | (–)8.92   | 7.5                     |
| Pro <sup>3</sup>  | –                    | 4.09         | 2.25, 1.91  | 2.02, 2.02   | 3.64, 3.64   | –      | –   | –                       |
| Gly <sup>4</sup>  | 8.46                 | 3.97, 3.88   | –           | –            | –            | –      | (–)5.42   | 5.8                     |
| Ser <sup>5</sup>  | 8.12                 | 4.72         | 3.86, 3.86  | –            | –            | –      | (–)4.89   | 6.5                     |
| Pro <sup>6</sup>  | –                    | 4.39         | 2.25, 1.85  | 2.02, 2.02   | 3.83, 3.71   | –      | –   | –                       |
| Gly <sup>7</sup>  | 8.50                 | 3.74, 3.74   | –           | –            | –            | –      | (–)7.78   | 6.0                     |
| Tyr <sup>8</sup>  | 7.97                 | 4.40         | 3.03, 2.91  | –            | –            | –      | (–)4.94   | 6.0                     |
| Tyr-Ser-Pro-D-Ala-Ser-Pro-D-Ala-Tyr-NH <sub>2</sub> (3) |                      |              |             |              |              |        |   |                         |
| Tyr <sup>1</sup>  | –                    | 4.24         | 3.05, 3.05  | –            | –            | –      | –   | –                       |
| Ser <sup>2</sup>  | 8.60                 | 4.74         | 3.85, 3.72  | –            | –            | –      | (–)8.38   | 7.5                     |
| Pro <sup>3</sup>  | –                    | 4.14         | 2.25, 1.89  | 2.06, 2.06   | 3.66, 3.66   | –      | –   | –                       |
| D-Ala <sup>4</sup>                                      | 8.49                 | 4.32         | 1.37        | –            | –            | –      | (–)7.04   | 6.5                     |
| Ser <sup>5</sup>  | 8.07                 | 4.74         | 3.85, 3.85  | –            | –            | –      | (–)4.24   | 7.5                     |
| Pro <sup>6</sup>  | –                    | 4.37         | 2.25, 1.87  | 2.06, 2.06   | 3.85, 3.77   | –      | –   | –                       |
| D-Ala <sup>7</sup>                                      | 8.41                 | 4.10         | 1.11        | –            | –            | –      | (–)8.97   | 6.5                     |
| Tyr <sup>8</sup>  | 8.15                 | 4.38         | 3.06, 2.83  | –            | –            | –      | (–)5.74   | 6.0                     |
| Tyr-Ser-Pro-Gly-Ser-Pro-Ser-Tyr-NH <sub>2</sub> (4)     |                      |              |             |              |              |        |   |                         |
| Tyr <sup>1</sup>  | –                    | 4.23         | 3.10, 3.10  | –            | –            | –      | –   | –                       |
| Ser <sup>2</sup>  | 8.58                 | 4.73         | 3.72, 3.72  | –            | –            | –      | (–)8.16   | 7.0                     |
| Pro <sup>3</sup>  | –                    | 4.28         | 2.30, 1.95  | 2.00, 2.00   | 3.69, 3.69   | –      | –   | –                       |
| Gly <sup>4</sup>  | 8.53                 | 3.94, 3.94   | –           | –            | –            | –      | (–)7.53   | 6.0                     |
| Ser <sup>5</sup>  | 8.15                 | 4.74         | 3.84, 3.84  | –            | –            | –      | (–)5.94   | 7.0                     |
| Pro <sup>6</sup>  | –                    | 4.40         | 2.20, 1.72  | 1.98, 1.98   | 3.80, 3.70   | –      | –   | –                       |
| Ser <sup>7</sup>  | 8.38                 | 4.30         | 3.70, 3.70  | –            | –            | –      | (–)7.26   | 7.0                     |
| Tyr <sup>8</sup>  | 8.10                 | 4.52         | 3.08, 2.93  | –            | –            | –      | (–)6.62   | 7.0                     |
| Tyr-Ser-Pro-Thr-Ser-Pro-Gly-Tyr-NH <sub>2</sub> (5)     |                      |              |             |              |              |        |   |                         |
| Tyr <sup>1</sup>  | –                    | 4.23         | 3.12, 3.06  | –            | –            | –      | –   | –                       |
| Ser <sup>2</sup>  | 8.54                 | 4.74         | 3.78, 3.78  | –            | –            | –      | (–)7.33   | 8.0                     |
| Pro <sup>3</sup>  | –                    | 4.36         | 2.32, 1.95  | 2.00, 2.00   | 3.71, 3.71   | –      | –   | –                       |
| Thr <sup>4</sup>  | 8.17                 | 4.30         | 3.11        | –            | –            | 1.18   | (–)6.67   | 8.0                     |
| Ser <sup>5</sup>  | 8.28                 | 4.74         | 3.78, 3.78  | –            | –            | –      | (–)7.03   | 6.5                     |
| Pro <sup>6</sup>  | –                    | 4.41         | 2.26, 1.88  | 2.01, 2.01   | 3.81, 3.81   | –      | –   | –                       |
| Gly <sup>7</sup>  | 8.49                 | 3.83, 3.83   | –           | –            | –            | –      | (–)7.20   | 5.5                     |
| Tyr <sup>8</sup>  | 8.02                 | 4.47         | 3.06, 2.94  | –            | –            | –      | (–)6.28   | 7.0                     |

<sup>a</sup> Chemical shift positions of the individual ring protons of the tyrosine residues are not reported.

specific residues in the primary sequence. There are four residues ( $i$  to  $i+3$ ) involved in a  $\beta$ -turn motif and for both  $\beta$ -turn types a strong  $d_{\text{NN}}(i+2, i+3)$  NOE connectivity is expected along with a  $d_{\alpha\text{N}}(i+1, i+3)$  connectivity which usually appears as a weak cross-peak in the ROESY spectrum. While  $d_{\text{NN}}(i, i+2)$  connectivities are generally unobserved in aqueous solutions (21), the presence of a weak  $d_{\text{NN}}(i+1, i+2)$  connectivity (when residues other than proline are present at the  $i+1$  position of a turn structure) distinguishes a type I turn from a type II turn, and the latter turn type exhibits a strong  $d_{\alpha\text{N}}(i+1, i+2)$  connectivity (27). Whenever a proline is present in a turn motif, the  $\delta$  protons show connectivities like an amide proton with neighboring residues. It should be pointed out, however, that these parameters, although necessary to identify a turn structure, are not unequivocal evidence making it difficult to further classify a  $\beta$ -turn structure as to its various type (i.e. type I vs. type II etc.). Thus, a combination NMR connectivities along with corroborating evidence provided by other forms of spectroscopy, such as CD, are necessary to determine unambiguously the presence of a  $\beta$ -turn.

In the present study the key evidence for the presence of  $\beta$ -turn structure was obtained from NOE patterns including  $d_{\text{NN}}$  connectivities and strong  $d_{\alpha\text{N}}(i+1, i+2)$  connectivities predicted to occur in such a motif. Furthermore, the temperature coefficients of the chemical shifts of backbone amide protons rendered information on the inter-residue hydrogen bonding patterns and their variations by residue replacement. In all the peptides studied, it was expected that the residues between 2 and 8 (amino acid residues are numbered sequentially from the amino-terminus to the carboxy-terminus of each peptide) form two overlapping Ser-Pro-Xaa-Xaa  $\beta$ -turn motifs (Fig. 2) in aqueous solution and, as expected, several of the abovementioned NOEs were observed.

While the peptide sequence found in **1** was the subject of a previous study (8), we elected also to examine its structure for direct comparison to our altered peptides. In our model of the native sequence (**1**) sequential NOEs ( $d_{\alpha\text{N}}$ ) were observed between residues 1–2, 3–4, 4–5, 6–7, 7–8, and  $d_{\alpha\delta}$  connectivities were observed between residues 2–3 and 5–6, permitting the sequence-specific assignment of the various amino acids present. Additionally, the observed  $d_{\text{NN}}$  (residues 4, 5) connectivity was somewhat weaker than the  $d_{\text{NN}}$  (residues 7, 8) connectivity, and there was a weak  $d_{\text{N}\delta}$  (residues 2, 3) connectivity observed, whereas such a connectivity was not present between residues 5 and 6. These NOE patterns suggest that the amino-terminal Ser-Pro-Xaa-Xaa sequence of **1** (residues 2–5) may be characterized as a mixture of type I and type II turn structure while the carboxy-

terminal Ser-Pro-Xaa-Xaa sequence (residues 5–8) forms a type II structure.

Overall, the amino-terminal Ser-Pro-Xaa-Xaa sequence of the molecule exhibits weak NOEs in comparison to the carboxy-terminal Ser-Pro-Xaa-Xaa sequence, most likely due to additional internal motion resulting from the dynamic interconversion between a mixture of the two types of turns that are present in aqueous solution. The  $^3J_{\text{HN}\alpha}$  coupling constant for the third residue in the amino-terminal turn (Thr<sup>4</sup>) was 8.0 Hz which is closer to that observed for a type I turn while that of Ser<sup>7</sup> was 7.0 Hz which is slightly larger than the 5 Hz value expected for a type II turn. The temperature coefficients of all the observable backbone amide protons were ca. (–)7.5 ppb/K, indicating that all residues are equally exposed to the solvent and that intramolecular hydrogen bonding, as would be predicted to occur between the  $i$  and  $i+3$  residues of an individual  $\beta$ -turn, is weak. These findings suggest that, despite the small size of the peptide, there is a low, but nonetheless observable, population of ordered structure in the form of two  $\beta$ -turns in aqueous solution, as noted previously (8).

The structural stability of the ‘next generation’ of peptides (**2–5**) was assessed by the same NMR methods discussed above. Although NOE intensities were not used quantitatively to estimate folded populations, they were used qualitatively to compare the stabilization of the folded structures found within this closely related family of peptides. As shown in Fig. 6, the ROESY spectrum of **2**, which contained glycine at the  $i+2$  positions of each  $\beta$ -turn-forming unit in place of Thr<sup>4</sup> and Ser<sup>7</sup> found in the native sequence, shows NOEs characteristic of a type II  $\beta$ -turn secondary structure for both halves of the molecule; compared to the native sequence, both the  $d_{\text{NN}}(i+2, i+3)$  NOE connectivities were relatively strong and about the same intensity within this peptide. The fingerprint (NH-C $\alpha$ H) region (Fig. 6) shows all sequential NOE connectivities and, in addition, that the  $d_{\alpha\text{N}}(i+1, i+2)$  connectivities are stronger than the corresponding  $d_{\alpha\text{N}}(i+2, i+3)$  connectivities further indicating a type II  $\beta$ -turn structure (27).

In conjunction with this connectivity data, the temperature coefficients of the amide protons of residues 5 and 8 of **2** were found to be (–)4.89 and (–)4.94 ppb/K, respectively, accompanied by low values of  $^3J_{\text{HN}\alpha}$  coupling constants for residues 4 and 7 (5.8 Hz and 6.0 Hz respectively). The relatively low temperature coefficients for the amide protons of **2** in comparison to **1**, along with the low coupling constants, provide strong evidence for the stabilization of type II  $\beta$ -turns within both the amino- and carboxy-terminal Ser-Pro-Xaa-Xaa sequences of this peptide.

In peptide **3**, which replaced residues Thr<sup>4</sup> and Ser<sup>7</sup> with D-Ala, of the two  $d_{\text{NN}}(i+2, i+3)$  connectivities

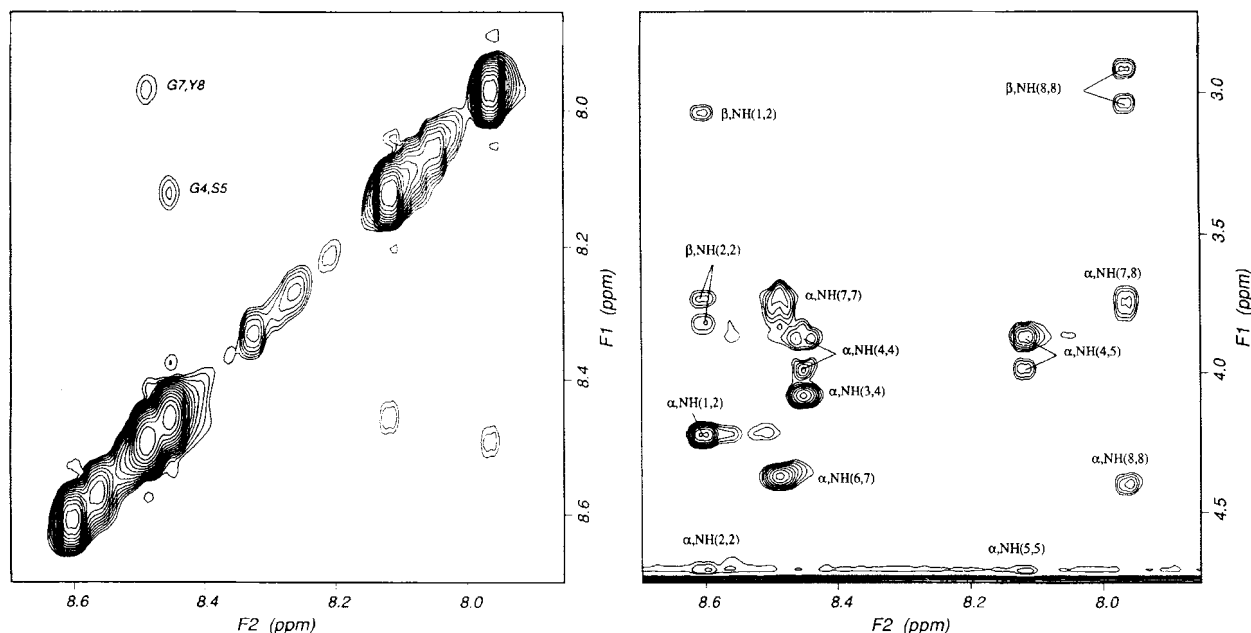


FIGURE 6

Portions of the 500 MHz proton ROESY spectrum of peptide **2** showing NOE connectivities in the NH-NH region (left panel) and in the NH-C $\alpha$ H region (right panel).

observed, the  $d_{\text{NN}}$ (residues 7, 8) connectivity was weaker than that of  $d_{\text{NN}}$ (residues 4, 5) (Fig. 7). In addition, stabilization of the  $i$  to  $i+3$  hydrogen bonds of the peptide were indicated by the relatively low temperature coefficient values of  $(-)$ 4.24 ppb/K for

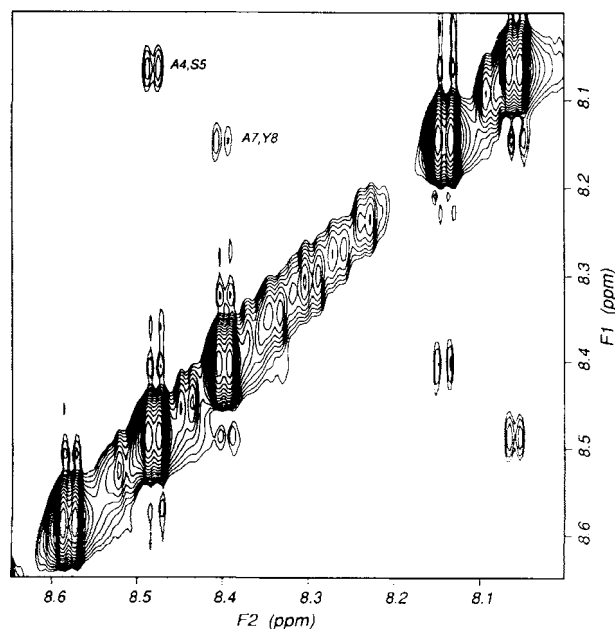


FIGURE 7

A portion of the 500 MHz proton ROESY spectrum of peptide **3** showing NH-NH NOE connectivities.

Ser<sup>5</sup> in the amino-terminal Ser-Pro-Xaa-Xaa sequence and  $(-)$ 5.74 ppb/K for the Tyr<sup>8</sup> amide proton in the carboxy-terminal Ser-Pro-Xaa-Xaa sequence. The  $^3J_{\text{HN}\alpha}$  coupling constants of the D-Ala residues at the 4 and 7 positions were also lowered to a value of about 6.0 Hz. Based on these data it is reasonable to suggest that both halves of peptide **3**, like **2**, adopt a type II  $\beta$ -turn and that the turn structure in the amino-terminal Ser-Pro-Xaa-Xaa site is stabilized to a greater extent in comparison to the carboxy-terminal site.

Overall, the NMR data indicates that substitution of the  $i+2$  position of each Ser-Pro-Xaa-Xaa sequence promotes the formation of type II  $\beta$ -turns, as also supported by our CD measurements. In addition, the NMR data have also permitted an evaluation of the extent of stabilization attributed to each individual Ser-Pro-Xaa-Xaa  $\beta$ -turn of a peptide and suggests that each site responds differently to the stabilizing influence of either a Gly or D-Ala substitution.

In order to investigate further the possible influence of turn stabilization in one Ser-Pro-Xaa-Xaa site on the other *unsubstituted* Ser-Pro-Xaa-Xaa site, peptides **4** and **5**, containing the single substitutions of glycine at position 4 or 7 of the native sequence, were again examined; glycine substitutions were chosen over D-Ala substitutions due to the relatively strong NOE connectivities observed in **2**. Peptide **4**, which differs from the native sequence at only position 4, showed NOE connectivities (mainly  $d_{\text{NN}}$ ) characteristic of a

type II turn for both the amino-terminal and carboxy-terminal Ser-Pro-Xaa-Xaa sites. Further, the  $^3J_{\text{HN}\alpha}$  coupling constant for Gly<sup>4</sup> was 6.0 Hz and that in Ser<sup>7</sup> was 7.0 Hz compared to the values of 8.0 Hz and 7.0 Hz observed for the 4 and 7 positions of peptide 1, respectively. Additionally, the temperature coefficient of the Ser<sup>5</sup> amide proton of **4** was (-)5.94 ppb/K indicating that the Gly substitution, as expected, favored the formation of a  $\beta$ -turn within the amino-terminal portion of the peptide. However, it was observed that this Gly substitution *also* promoted hydrogen bonding between Ser<sup>5</sup> and Tyr<sup>8</sup> in the second half of the peptide as evidenced by the reduced temperature coefficient of the amide proton of Tyr<sup>8</sup> [(-)6.62 ppb/K] as compared to the value of (-)7.65 ppb/K in peptide 1. It is thus reasonable to speculate that substitution of Gly at position 4 of the peptide stabilized the type II turn in the amino-terminal half *which also influenced* the stability of the turn structure in the carboxy-terminal (unsubstituted) half of the peptide.

Similarly, peptide **5**, which differs from the native sequence only at position 7, showed typical type II  $\beta$ -turn NOE patterns and temperature coefficients for the Ser<sup>5</sup> and Tyr<sup>8</sup> amide protons [(-)7.03 and (-)6.28 ppb/K, respectively] and  $^3J_{\text{HN}\alpha}$  coupling constants of 8.0 Hz and 5.5 Hz for Thr<sup>4</sup> and Gly<sup>7</sup>, respectively. These data suggest that, unlike the Gly substitution at position 4 which stabilizes the turn structure within *both* the amino-terminal and carboxy-terminal Ser-Pro-Xaa-Xaa sequences, the substitution at position 7 stabilizes only the turn structure in which it resides.

#### Molecular modeling

The spectroscopic data presented indicate that the secondary structure of peptides **2** and **3** consist of two, overlapping type II  $\beta$ -turns. Thus, as observed previously (21), the stabilization of turn structures in peptides **2** and **3** may be attributed to the small size of Gly and the inverted C $_{\alpha}$  stereocenter of D-Ala which minimizes steric hindrance to turn formation in comparison to the relatively larger residues in the native sequence (Thr and Ser). These data enable reasonable models of **2** and **3** to be constructed containing type II  $\beta$ -turns within each of the overlapping Ser-Pro-Xaa-Xaa sites. Using the accepted (20) backbone torsion angles for a type II turn ( $\phi_{i+1}$ ,  $\psi_{i+1}$ ) = (-60°, +120°) ( $\phi_{i+2}$ ,  $\psi_{i+2}$ ) = (+80°, 0°), structures can be generated that indicate the formation of rather compact, folded peptides (e.g. peptide **2**, Fig. 8). This observation is further substantiated by the relatively low temperature coefficients of the amide protons of the substituted Gly residues in **2** [(-)5.8 ppb/K at position 4 and (-)6.0 ppb/K at position 7] which indicate that this residue is screened from solvent much more effectively than the corresponding residues in the native peptide (Table 1); a similar argument can also be applied to the D-Ala

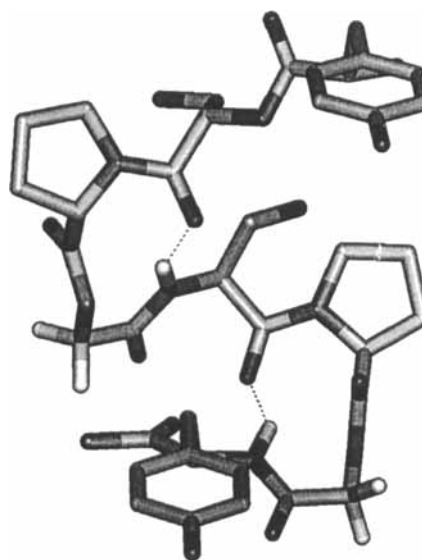


FIGURE 8

Molecular model of peptide **2** containing two type II  $\beta$ -turns based on spectroscopic evidence (CD and NMR).

substituted peptide **3** which again favors *i* to *i*+3 hydrogen bonding and stabilizes the turn structure.

Overall, the model (Fig. 8) not only illustrates the compact nature and spatial arrangement of tandem type II  $\beta$ -turns, but also emphasizes that the pre-organized structures which result can potentially orient the aromatic moieties of the sequence in a fashion suitable for bis-intercalation of DNA. In addition, analysis of the model reveals that with the aromatic rings positioned as shown, multiple hydrogen bond donor and acceptor sites are poised for intimate contact with the grooves of a DNA helix; this property of the structure could lead to DNA binding selectivity as observed with the quinoxaline antibiotics (7). While DNA binding in the presence of the native Tyr residues alone is expected to be relatively weak (9), the model appears to be consistent with the idea that the overlapping  $\beta$ -turn systems developed herein may assist in creating a linking system, in conjunction with *alternative* aromatic residues (29), for the construction of novel bis-intercalators.

#### CONCLUSIONS

The investigations described above have explored the use of amino acid substitutions to impart structural preorganization to a unique *tandem*  $\beta$ -turn forming motif. The experiments performed have demonstrated that substitution of either Gly or D-Ala was sufficient to induce a relatively high population of type II  $\beta$ -turns within these overlapping motifs in contrast to the native motif sequence. Additionally, study of mono-substituted peptides suggests that stabilizing a

$\beta$ -turn within the amino-terminal portion of the tandem structure supports the formation of the  $\beta$ -turn immediately to its carboxy side, whereas inducing  $\beta$ -turn structure within the carboxy-terminal portion only affects the Ser-Pro-Xaa-Xaa sequence in which it resides.

The findings outlined herein are significant in several regards. First, they demonstrate the wherewithal to transform a native DNA-binding protein sequence into a structurally preorganized motif that may provide the basis, in conjunction with the modification of the aromatic moieties (29), for new DNA binding bisintercalators having unique site-selectivities and biological activities. Secondly, these data explore, and improve upon, the structure of a naturally occurring protein motif consisting of tandem repeats of  $\beta$ -turns (30); the data presented may, in the future, assist in applying such motifs in the development of *de novo* designed proteins or oligopeptides.

### ACKNOWLEDGEMENTS

We thank the National Institutes of Health (GM 50557) for financial support of this work. Additionally, we also thank Dr. Daniel Robertson of the Chemistry Department's Computational Molecular Science Facility for assistance in molecular modeling and the IUPUI Research Investment Fund for instrument support (circular dichroism).

### REFERENCES

- Churchill, M.E.A. & Travers, A.A. (1991) *Trends Biochem. Sci.* **16**, 92–97
- (i) Suzuki, M. (1989) *EMBO J.* **8**, 797–804; (ii) Suzuki, M. (1989) *J. Mol. Biol.* **207**, 61–84; (iii) Churchill, M.E.A. & Suzuki, M. (1989) *EMBO J.* **8**, 4189–4195; (iv) Bailly, F., Bailly, C., Waring, M.J. & Henichart, J.-P. (1992) *Biochem. Biophys. Res. Commun.* **184**, 930–937
- (i) Reeves, R. & Nissen, M.S. (1990) *J. Biol. Chem.* **265**, 8573–8582; (ii) Geierstanger, B. H., Volkman, B. F., Kremer, W. & Wemmer, D.E. (1994) *Biochemistry* **33**, 5347–5355
- Zimmer, C. & Wahnert, U. (1986) *Progr. Biophys. Mol. Biol.* **47**, 31–112
- (i) Young, R.A. (1991) *Annu. Rev. Biochem.* **60**, 689–715; (ii) Corden, J.L. (1990) *Trends Biochem. Sci.* **15**, 383–387; (iii) Woychik, N.A. & Young, R.A. (1990) *Trends Biochem. Sci.* **15**, 347–350
- Suzuki, M. (1990) *Nature (London)* **344**, 562–565
- (i) Waring, M.J. & Wakelin, L.P.G. (1974) *Nature (London)* **252**, 653–657; (ii) Quigley, G. J., Ughetto, G., van der Marel, G. A., van Boom, J. H., Wang, A. H.-J. & Rich, A. (1986) *Science* **232**, 1255–1258
- Harding, M.M. (1992) *J. Med. Chem.* **35**, 4658–4664
- Huang, X., Shullenberger, D.F. & Long, E.C. (1994) *Biochem. Biophys. Res. Commun.* **198**, 712–719
- Serizawa, H., Conaway, R.C. & Conaway, J.W. (1993) *J. Biol. Chem.* **268**, 17300–17308
- (i) Kim, W.K. & Dahmus, M.E. (1986) *J. Biol. Chem.* **261**, 14219–14225; (ii) Cadena, D.L. & Dahmus, M. E. (1987) *J. Biol. Chem.* **262**, 12486–12474; (iii) Zhang, J. & Corden, J.L. (1991) *J. Biol. Chem.* **266**, 2290–2296; (iv) Zhang, J. & Corden, J.L. (1991) *J. Biol. Chem.* **266**, 2297–2302
- Kelly, W. G., Dahmus, M.E. & Hart, G.W. (1993) *J. Biol. Chem.* **268**, 10416–10424
- Stewart, J.M. & Young, J.D. (1984) *Solid Phase Peptide Synthesis*. Pierce Chemical Co., Rockford, IL
- Tam, J.P. & Merrifield, R.B. (1987) *The Peptides: Analysis, Synthesis, and Biology*, vol. 9, pp. 185–248, Academic Press, New York
- Yajima, H. & Fujii, M. (1983) *The Peptides: Analysis, Synthesis, and Biology*, vol. 5, pp. 65–109, Marcel-Dekker, New York
- States, D. J., Haberkon, R.A. & Ruben, D.J. (1982) *J. Magn. Reson.* **48**, 286–292
- Piantini, U., Sorensen, O.W. & Ernst, R.R. (1982) *J. Am. Chem. Soc.* **104**, 6800–6801
- Bothner-By, A. A., Stephens, R.L. & Lee, J. (1981) *J. Am. Chem. Soc.* **103**, 3654–3658
- Bax, A. & Davis, D.G. (1985) *J. Magn. Res.* **63**, 207–213
- (i) Chou, P. & Fasman, G.D. (1977) *J. Mol. Biol.* **115**, 135–175; (ii) Wilmot, C.M. & Thornton, J.M. (1988) *J. Mol. Biol.* **203**, 221–232
- Imperiali, B., Fisher, S. L., Moats, R.A. & Prins, T. J. (1992) *J. Am. Chem. Soc.* **114**, 3182–3188
- Perczel, A., Hollosi, M., Foxman, B.M. & Fasman, G.D. (1991) *J. Am. Chem. Soc.* **113**, 9772–9784
- Woody, R.W. (1974) in *Peptides, Polypeptides and Proteins* (Blout, E. R., Bovey, F. A., Lotan, N. and Goodman, M., eds.), pp. 338–350, Wiley, New York
- Perczel, A., Hollosi, M., Sandor, P. & Fasman, G.D. (1993) *Int. J. Peptide Protein Res.* **41**, 223–236
- Lisowski, M., Pietrzynski, G. & Rzeszotarska, B. (1993) *Int. J. Peptide Protein Res.* **42**, 466–474
- Kumar, A., Ernst, R.R. & Wuthrich, K. (1980) *Biochem. Biophys. Res. Commun.* **96**, 1156–1163
- Wuthrich, K. (1986) *NMR of Proteins and Nucleic Acids*, Wiley, New York
- Dyson, H. J., Rance, M., Houghten, R. A., Lerner, R.E. & Wright, P.E. (1988) *J. Mol. Biol.* **201**, 161–200
- Huang, X. & Long, E.C. (1995) *Biomed. Chem. Lett.* **5**, 1937–1940
- Cagas, P.M. & Corden, J.L. (1995) *Proteins: Struct. Funct. Gen.* **21**, 149–160

Address:

Prof. Eric C. Long  
 Department of Chemistry  
 Indiana University Purdue University-Indianapolis  
 402 North Blackford Street  
 Indianapolis, IN 46202-3274  
 USA

Telephone: (317) 274-6888

Fax: (317) 274-4701